Normal State ac Hall Effect in $YBa_2Cu_3O_7$ Thin Films

S. G. Kaplan, S. Wu, H.-T. S. Lihn, and H. D. Drew
Laboratory for Physical Sciences, College Park, Maryland 20740
and Center for Superconductivity Research, Department of Physics, University of Maryland, College Park, Maryland 20742

Q. Li and D. B. Fenner
Advanced Fuel Research, East Hartford, Connecticut 06138

Julia M. Phillips* and S. Y. Hou
AT&T Bell Laboratories, 600 Mountain Avenue, Murray Hill, New Jersey 07974
(Received 31 July 1995)

We have measured the magnetotransmission of thin film samples of $YBa_2Cu_3O_7$ in the normal state using circularly polarized light at frequencies from 15 to 180 cm^{-1}. The magneto-optical signal is consistent with the ac Hall effect of holes with a reduced scattering rate and an enhanced mass compared to the zero-field transport parameters. This result agrees with a simple high-frequency extension of models which have been developed to explain the anomalous dc Hall effect in the normal state of high-T_c superconductors.

PACS numbers: 78.20.Ls, 72.15.Gd, 74.72.Bk

The nature of the *ab*-plane charge carrier dynamics in the normal state of $YBa_2Cu_3O_7$ is currently as intriguing a subject as the mechanism responsible for the superconductivity below T_c. Hall measurements have revealed the charge carriers to be holes with a density related to the oxygen doping level, but there the resemblance to simple metals ends. A striking T^2 behavior of the inverse Hall angle $\cot\theta_H = \sigma_{xx}/\sigma_{xy}$ has been observed in many different types of samples [1–4]. In addition, the ac conductivity, derived from broadband optical reflectivity measurements [5,6], shows distinctly non-Drude-like behavior above 200 cm^{-1}. On the other hand, previous far-infrared (FIR) magnetotransmission measurements of $YBa_2Cu_3O_7$ in the superconducting state [7] have found a signal consistent with cyclotron resonance of free holes with a mass m_c of $(3.1 \pm 0.5)m_e$.

In this Letter we measure the FIR magneto-optical activity of $YBa_2Cu_3O_7$ thin films at 9 T and 95 K, where $\omega_c\tau \sim 1/40$, so that we observe an overdamped cyclotron resonance response, or more appropriately the ac Hall effect. The signal is consistent with a holelike Hall effect, but fitting the data with a Drude model requires a smaller scattering rate and larger mass then the zero-field values. This result is understood by extending the ideas of Anderson [1,2] or Carrington *et al.* [3,4], used to explain the temperature dependence of the dc Hall effect, to high frequencies. In these theories, the Hall effect is dependent upon a scattering time and mass which are distinct from the ordinary transport quantities and are associated with spinons, or carriers near the corners of the 2D Fermi surface, respectively. Other phenomenological theories have also been proposed to explain the appearance of two scattering times in the charge dynamics of cuprate materials [8].

Two types of thin film samples were used in these studies. High quality films of $YBa_2Cu_3O_7$ were produced by precursor deposition onto (100) $LaAlO_3$ substrates, followed by postannealing at 800 °C in a wet oxygen atmosphere. Such films have proven to be of higher quality than typical laser-deposited samples, in terms of their degree of crystallinity and low defect density [9]. The superconducting transitions were characterized by dc resistivity and ac susceptibility measurements and found to be typically 92 ± 0.3 K. Another class of samples were grown by pulsed laser deposition and *in situ* annealing on Si substrates with a buffer layer of yttria-stabilized zirconia. These samples had transitions typically of 89 ± 0.5 K.

FIR magnetotransmission measurements from 15 to 200 cm^{-1}, in the Faraday geometry, were performed with a polarizing Michelson interferometer above 30 cm^{-1}, and with several lines from an optically pumped FIR laser below 55 cm^{-1}, in conjunction with a 4.2 K Si bolometric detector. The samples were held in the bore of a superconducting 9 T magnet on a movable stage, allowing the transmission of a sample to be compared to that of a blank substrate for absolute transmission measurements. A circular polarizer, consisting of a linear polarizer and a 0.53-cm-thick x-cut quartz wave plate, was calibrated using cyclotron resonance in GaAs and InAs quantum well structures. The magneto-optical activity of the samples was "unfolded" from the raw signal using the measured polarizer calibration curve, as described earlier [7,10]. Since the complex index of refraction, $n + ik$, of $LaAlO_3$ is highly frequency and temperature dependent in this spectral region, separate characterizations were performed for these substrates, using a scanning high-resolution interferometer to measure the Fabry-Pérot fringe spacings, as

 0031-9007/96/76(4)/696(4)$06.00

well as the attenuation, in order to obtain n and k versus frequency at different temperatures.

Figure 1(a) shows as the solid circles the transmittance ratio $T(+8.9\ \mathrm{T})/T(-8.9\ \mathrm{T})$ in circularly polarized light for a $YBa_2Cu_3O_7$ film of thickness $d_f = 500$ Å on $LaAlO_3$ at 95 K. Figure 1(b) shows the zero-field transmission relative to a blank piece of $LaAlO_3$. The magneto-optical activity spectrum in Fig. 1(a) has a peak near 80 cm^{-1}, while the 0-field spectrum shows a characteristic Drude frequency dependence. The solid curves in each frame show fits by a simple Drude model (using the standard sheet conductance formula for the film and treating the multiple reflections in the substrate incoherently) for a dc sheet resistance $R_\square$ of 20.4 Ω and scattering rate $\tau_{\mathrm{tr}}^{-1} = 127\ cm^{-1}$. This is the minimum value for τ_{tr}^{-1} that is consistent with the data. In frame (a), however, the peak in the solid curve fit is near 110 cm^{-1}, clearly at higher frequency than the peak in the data. In this fit, we have chosen the carrier mass $m_{\mathrm{tr}} = 3.0$ from previous estimates of FIR measurements [5,6]. However, varying the carrier mass changes only the amplitude, not the peak position of the fit.

The normal state magneto-optic response was also measured for a 400 Å thick $YBa_2Cu_3O_7$ film on Si, shown in Fig. 2. The solid circles show $T(+8.9\ \mathrm{T})/T(-8.9\ \mathrm{T})$ in Fig. 2(a) and the 0-field transmission in Fig. 2(b). The gaps in each frame near 130 cm^{-1} are due to a phonon in the quartz wave plate. Again the 0-field data are fit with a Drude model, in this case with parameters $R_\square = 25.9$ Ω and $\tau_{\mathrm{tr}}^{-1} = 190\ cm^{-1}$. The resulting fits are shown as the solid curves in both frames. In frame (b), the Drude curve provides an excellent fit, with the small structures near 120, 155, and 190 cm^{-1} likely coming from optic phonons in $YBa_2Cu_3O_7$. However, the solid curve in Fig. 2(a), calculated with $m_{\mathrm{tr}} = 3.0$, has a peak near 170 cm^{-1}, compared to the data which has a peak near 60 cm^{-1}. In both samples, the magneto-optical activity shows an approximately Drude-like frequency response, but with a smaller scattering rate than the 0-field conductivity.

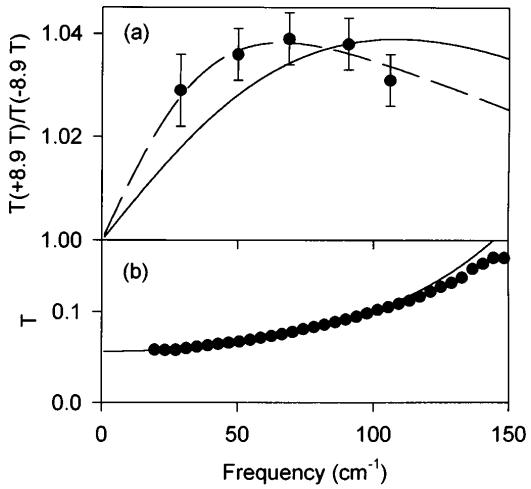

FIG. 1. FIR transmission spectra for a 500 Å $YBa_2Cu_3O_7$ film on $LaAlO_3$ at 95 K. (a) Ratio of the transmittance at +8.9 to −8.9 T with circularly polarized light. The solid circles show the data, the solid line is the prediction of the Drude model with parameters used to fit the 0-field data in (b), and the dashed line is a fit by the conductivity formula in Eq. (2). (b) 0-field transmittance of the sample ratioed to a bare substrate. The solid circles are the data, and the solid curve a fit by a Drude conductivity with parameters listed in the text.

These seemingly anomalous results can be understood by using a high-frequency extension of models which have been used to explain the T^2 dependence of the normal state inverse Hall angle σ_{xx}/σ_{xy} observed in dc transport measurements. In Anderson's model [1] for the normal state of high-T_c superconductors, σ_{xx} has the ordinary form, $\propto \tau_{\mathrm{tr}}$, the decay time for holons scattering from thermally excited spinons. On the other hand, σ_{xy} depends on both τ_{tr} and the scattering time of spinon excitations, τ_H: $\sigma_{xy} \propto \tau_{\mathrm{tr}}\tau_H$. The decay rate for holons, τ_{tr}^{-1}, depends on the number of thermally excited spinons, and so is proportional to T, while the scattering rate for spinons, τ_H^{-1}, depends upon magnetic impurity and spinon-spinon scattering and goes like $A + BT^2$.

An alternative model, put forward by Carrington and co-workers [3,4], explains the same temperature dependence within a model involving Fermi surface (FS) anisotropy in the a-b plane. It has been pointed out, however, that their assumption that $l_1 \gg l_2$, where l_1 and l_2 are the mean free paths at the corners and along the edges of the FS, may not hold [11] for the wide variety of high-T_c materials that show the T^2 dependence in $\cot\theta_H$. In fact the ratio of the mean free paths is estimated [4] to be only ~3 for $YBa_2Cu_3O_7$.

It is not clear how to extend either of these models to finite frequency in a rigorous manner. Romero [12] postulated a simple form for the mobility tensor and

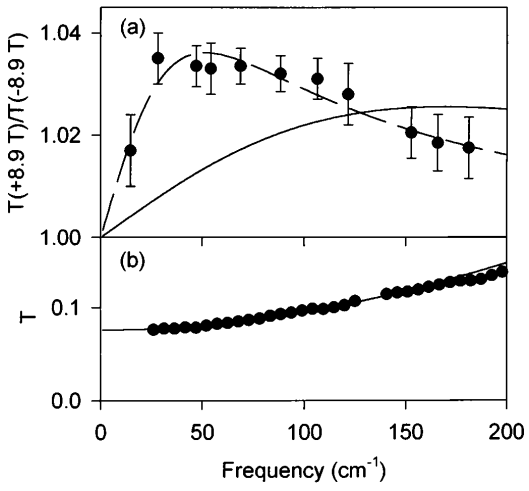

FIG. 2. FIR transmission spectra for a 400 Å $YBa_2Cu_3O_7$ film on Si at 95 K. See the caption for Fig. 1 for descriptions of the various curves. Note that the difference between the Drude curve and the data in (a) is more pronounced for this sample than the $LaAlO_3$ sample shown in Fig. 1.

extended Anderson's model in the following way:

$$\sigma_{\pm} = \frac{n_c e^2 \tau_{\rm tr}}{m_{\rm tr}} \frac{1}{1 - i\omega\tau_{\rm tr} \pm i\omega_c \tau_H}, \qquad (1)$$

where n_c is the carrier density, $m_{\rm tr}$ is the transport mass (for motion perpendicular to the FS), and $\omega_c = eH/m_H c$, with a cyclotron mass m_H (for motion parallel to the FS). Equation (1) describes a Drude Hall effect with the cyclotron frequency shifted to $\omega_c \tau_H/\tau_{\rm tr}$, but with the same scattering rate as the zero-field response. We note that Eq. (1) can also be "derived" from a Boltzmann equation approach in the relaxation time approximation by associating τ_H with the Lorentz force term and $\tau_{\rm tr}$ with the other terms. As it stands, this result will not fit the data in Fig. 1, but if we assume that $1/\tau_H \propto A + B'\omega^2$, in keeping with a Fermi liquid approach, then the optical activity will be enhanced at low frequency relative to the simple Drude model. However, the required value of $B' \sim 0.006$ cm is more than an order of magnitude larger than that estimated from the temperature dependence of the dc Hall angle data [assuming that the scattering rate is proportional to $(\pi kT)^2 + \omega^2$].

Another approach, which can be used to extend either Anderson's or the FS result to high frequency in the weak field limit, is to replace τ_H and $\tau_{\rm tr}$ in the expression for σ_{xx} and σ_{xy} with $\tau_H^* = \tau_H/(1 - i\omega\tau_H)$ and $\tau_{\rm tr}^* = \tau_{\rm tr}/(1 - i\omega\tau_{\rm tr})$, respectively. This form is easily justified in the FS models. In the case of two-excitation models such as Anderson's it can be expected from two coupled Boltzmann equations. This approach leads to the following conductivity function:

$$\sigma_{\pm} = \frac{n_c e^2 \tau_{\rm tr}}{m_{\rm tr}} \frac{1}{1 - i\omega\tau_{\rm tr}} \left[1 \pm \frac{i\omega_c \tau_H}{1 - i\omega\tau_H} \right], \qquad (2)$$

where again $\omega_c = eH/m_H c$. Both this function and that in Eq. (1) reduce to Anderson's or the FS result at zero frequency, a simple Drude model if $\tau_H = \tau_{\rm tr}$ and $m_H = m_{\rm tr}$, and obey causality and the oscillator strength sum rule. The form in Eq. (2), however, predicts a non-Drude form of the ac Hall signal, with a roll-off frequency given approximately by $1/\tau_H$, distinct from the decay rate for transport currents.

The dashed line in Fig. 1(a) shows a fit by the conductivity function of Eq. (2) with $\tau_H^{-1} = 68 \pm 10$ cm^{-1} and $m_H = (5.2 \pm 0.7) m_e$, indicating $\tau_H \sim 2\tau_{\rm tr}$ and $m_H \sim 2m_{\rm tr}$. This fit can be taken as direct evidence for the presence of two distinct scattering rates in the normal state electrodynamics of $YBa_2Cu_3O_7$, with the scattering rate associated with the ac Hall effect being much smaller than the transport scattering rate. Within the Anderson picture, we can interpret the parameters m_H and τ_H as the spinon mass and scattering time, respectively. Interpreting the parameters in terms of l_1 and l_2 in the anisotropic FS model, we conclude that the two mean free paths differ by only ~50%, which seems to violate the geometric constraint used to motivate this picture.

Qualitatively similar results are found for the Si substrate sample shown in Fig. 2. The dashed line in Fig. 2(a) shows a fit by the conductivity function of Eq. (2), with $\tau_H^{-1} = 52 \pm 10$ cm^{-1} and $m_H = (6.6 \pm 0.8) m_e$. Thus the addition of a distinct scattering time and mass for the cyclotron resonance provides a quantitative fit to the magneto-optical data on both samples, with $\omega_c \tau_H$ equal to within 3%. However, the value of τ_H^{-1} for the Si sample is somewhat smaller than that found in the $LaAlO_3$ sample, even though $\tau_{\rm tr}^{-1}$ derived from the zero-field transmission of this sample is larger than the value for the $LaAlO_3$ sample. Because of the differing microtextures of these two types of samples, with large-scale defects such as grain boundaries and occlusions [9], it is difficult to predict how the different scattering processes should vary from sample to sample.

An alternative to fitting the data in Fig. 2(a) with the function in Eq. (2) is to derive the Hall conductivity by applying Kramers-Kronig analysis to the transmission data. In our case the field ratio $T(H)/T(0)$ for linearly polarized light (obtained from averaging the two circular polarizations) is different from 1 by less than 1%, so we can conclude that σ_{xx} is almost unchanged from the zero-field value and use the $T(+H)/T(-H)$ data to evaluate σ_{xy}, through the standard sheet conductance formula [13]

$$\frac{T(+H)}{T(-H)} = \frac{|1 + n + Z_0 \sigma^- d_f|^2}{|1 + n + Z_0 \sigma^+ d_f|^2}, \qquad (3)$$

where Z_0 is the impedance of free space. The zero-field σ_{xx} is evaluated from Kramers-Kronig analysis of the zero-field transmission data.

The results of this analysis are shown in Fig. 3 in terms of the real (solid circles) and imaginary (solid squares) parts of the Hall coefficient R_H. We have tried several high-frequency extrapolations and found little effect on the overall shape of the R_H curves below 150 cm^{-1}. In a simple Drude metal, the real part of R_H is frequency independent, given by $1/n_c ec$, and the imaginary part is zero. The clear frequency dependence of both quantities in our data is an indication of the non-Drude character of the charge dynamics in magnetic field for this material.

Also shown in Fig. 3 as the solid and dashed lines are the real and imaginary parts of R_H from Eq. (2) with the parameters used to fit the data in Fig. 2. These fits are sensitive to the value of n_c (for which we take the canonical value of 2.9×10^{-21} cm^{-3} corresponding to 0.25 hole per in-plane Cu) and to the effective film thickness, which is known to only ~25%. However, the fit to both components of R_H is as good as the fit to the transmission data in Fig. 2, providing a consistency check of both the model and the Kramers-Kronig analysis procedure. The value of 3.5×10^{-9} m^3/C for R_H at zero frequency and 95 K is comparable to published values for the dc Hall coefficient of single crystal $YBa_2Cu_3O_7$ with 1% Co impurity [3]. We note that the high-frequency limit of Eq. (2) yields $R_H(\omega \to \infty) = (m_{\rm tr}/m_H)/n_c ec$, implying that a high-frequency measurement of R_H could yield a value for the carrier density, which can only be guessed from the dc Hall effect data.

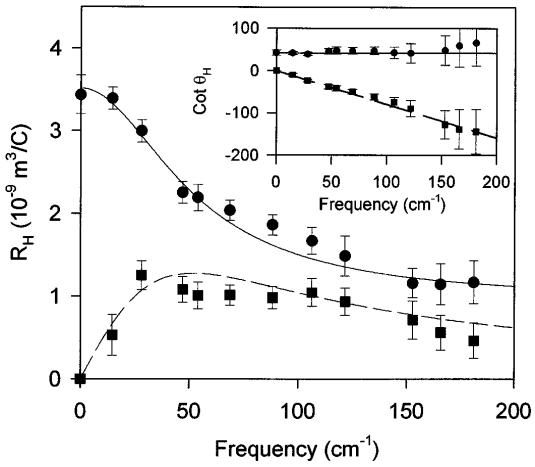

FIG. 3. Hall coefficient R_H vs frequency for the Si substrate sample. The solid circles and squares show, respectively, the real and imaginary parts of R_H derived from Kramers-Kronig analysis of the data in Fig. 2(a), while the solid and dashed curves show the predicted values from fitting Eq. (2) to the same data. Inset: Real (circles) and imaginary (squares) parts of $\cot\theta_H$, along with the predictions of Eq. (2) (solid and dashed lines). The real part is $1/\omega_c\tau_H$, and the slope of the imaginary part is $-1/\omega_c$.

The inset in Fig. 3 shows the real and imaginary parts of $\cot\theta_H$ derived for the Si substrate sample. The real part is almost constant within the error bars and is equal to $1/\omega_c\tau_H$ from Eq. (2). Our value of 40 for this quantity agrees well with the dc Hall angle data [2,3]. The imaginary part is given by $-\omega/\omega_c$, from which we derive $m_H = 6.6m_e$, in agreement with the fitted values by Eq. (2). The frequency independence of $\mathrm{Re}(\cot\theta_H)$ and the linear frequency dependence of $\mathrm{Im}(\cot\theta_H)$ are found in a simple Drude model and in some other models as well [8], with the exception of arbitrary two-band models. We take the values for m_H and τ_H derived from this plot as phenomenological definitions.

The conclusion that $m_H > m_{\mathrm{tr}} \approx m_c$ is consistent with the observation that the high frequency optical activity $T(+H)/T(-H) - 1$ is appreciably larger in the superconducting state [14] than in the normal state. However, it is expected on general grounds that the charge carriers should respond essentially as free holes at frequencies high enough that inertia dominates the dynamics. Therefore, this picture [Eq. (2)] should break down and the magneto-optical activity should become independent of temperature. What is this frequency scale? Evidently, it is not τ_H^{-1}. Also, it is apparently not τ_{tr}^{-1}, since Eq. (2) seems to fit the data well up to this frequency. This suggests that the appropriate scale may be the spin interaction energy $J \sim 0.2$ eV, or perhaps the superconducting gap energy, and that higher frequency magneto-optical measurements could be of interest.

Although the signal-to-noise ratio in the present experiment is inadequate to establish the precise power law for the temperature dependence of the magneto-optical signal, we have measured the signal for the Si sample up to 120 K at 28 and 54 cm^{-1} and found the temperature dependence to be quite rapid. At 54 cm^{-1}, the signal has decreased by more than a factor of 2 at 120 K. This seems to be at least as fast as a T^2 dependence for τ_H^{-1}.

In conclusion, the normal state optical activity spectra for $YBa_2Cu_3O_7$ at 95 K are inconsistent with a simple Drude ac Hall effect with a field-independent cyclotron mass and scattering rate. We fit the data with a simple finite frequency extension of models for the dc Hall effect. The results support the notion of an enhanced mass and reduced scattering rate for motion parallel to the FS compared to the longitudinal response. Within this model, we obtain $m_H = (6 \pm 1)m_e \sim (2 - 2.5)m_{\mathrm{tr}}$, with $\tau_H^{-1} = 60 \pm 15$ cm$^{-1} \sim (0.25 - 0.5)\tau_{\mathrm{tr}}^{-1}$.

We have enjoyed useful discussions with N. P. Ong, V. Yakovenko, A. Zheleznyak, D. B. Romero, and R. S. Decca. We would also like to thank M. Shayegan and R. Wagner for providing us with GaAs and InAs 2DEG samples for polarizer calibration. This work was supported in part by the National Science Foundation under Grant No. DMR 9223217.

*Present address: Sandia National Laboratories, Albuquerque, NM 87185.

[1] P. W. Anderson, Phys. Rev. Lett. **67**, 2092 (1991).
[2] T. R. Chien, Z. Z. Wang, and N. P. Ong, Phys. Rev. Lett. **67**, 2088 (1991); J. M. Harris, Y. F. Yan, and N. P. Ong, Phys. Rev. B **46**, 14 293 (1992).
[3] A. Carrington, A. P. Mackenzie, C. T. Lin, and J. R. Cooper, Phys. Rev. Lett. **69**, 2855 (1992).
[4] Chris Kendziora, David Mandrus, and Laszlo Mihaly, Phys. Rev. B **46**, 14 297 (1992).
[5] Joseph Orenstein, G. A. Thomas, A. J. Millis, S. L. Cooper, D. H. Rapkine, T. Timusk, L. F. Schneemeyer, and J. V. Waszczak, Phys. Rev. B **42**, 6342 (1990).
[6] L. D. Rotter, Z. Schlesinger, R. T. Collins, F. Holtzberg, C. Field, U. W. Welp, G. W. Crabtree, J. Z. Liu, Y. Fang, K. G. Vandervoort, and S. Fleshler, Phys. Rev. Lett. **67**, 2741 (1991).
[7] K. Karraï *et al.*, Phys. Rev. Lett. **69**, 355 (1992).
[8] P. Coleman, A. J. Schofield, and A. M. Tsvelik (to be published); V. Yakovenko (private communication); G. Kotliar, A. Sengupta, and C. M. Varma (to be published).
[9] M. P. Siegal *et al.*, J. Mater. Res. **7**, 2658 (1994); M. P. Siegal *et al.*, Appl. Phys. Lett. **60**, 2932 (1992); M. P. Siegal *et al.*, Appl. Phys. Lett. **60**, 2936 (1992).
[10] S. Wu, S. G. Kaplan, M. Quijada, K. Sengupta, and H. D. Drew, Rev. Sci. Instrum. (to be published).
[11] J. M. Harris, Y. F. Yan, N. P. Ong, and P. W. Anderson (to be published).
[12] D. B. Romero, Phys. Rev. B **46**, 8505 (1992).
[13] For the small signals that we observe, the right-hand side of Eq. (3) is given quite closely by the approximate form $1 + 4\,\mathrm{Im}(\sigma_{xy}/\sigma_{xx})$. The Kramers-Kronig analysis is thus essentially a linear transformation of the data.
[14] E.-J. Choi *et al.*, Phys. Rev. B **49**, 13 271 (1994).